

Ge tetramer structure of the $p(2\sqrt{2}\times 4\sqrt{2})R45^\circ$ surface reconstruction of Ge/Ag(001): A surface x-ray diffraction and STM study

H. Oughaddou, J.-M. Gay, B. Aufray, L. Lapena, and G. Le Lay

CRMC2, Centre National de la Recherche Scientifique, Campus de Luminy, Case 913, 13288 Marseille Cedex 09, France

O. Bunk, G. Falkenberg, J. H. Zeysing, and R. L. Johnson

Institut für Experimentalphysik, Universität Hamburg, Luruper Chaussee 149, D-22761 Hamburg, Germany

(Received 27 April 1999; revised manuscript received 29 September 1999)

The surface atomic structure of the $p(2\sqrt{2}\times 4\sqrt{2})R45^\circ$ superstructure obtained at 0.5-monolayer coverage by deposition of germanium on the Ag(001) surface at room temperature has been investigated using surface x-ray diffraction and scanning tunneling microscopy. A structural model is proposed with clusters of four Ge atoms preferentially adsorbed near hollow and bridge sites on the surface. The Ge-Ag bond strength is sufficient to induce rearrangement of the Ag atoms in the uppermost layers and stabilize the reconstruction.

I. INTRODUCTION

The structure and electronic properties of the interfaces formed by thin layers of noble metals deposited on semiconductor surfaces have been extensively studied over the past ten years.¹⁻⁴ This type of work is motivated by the technological necessity of understanding the electronic interface states and the details of the Schottky-barrier formation on semiconductors. Surprisingly, only very few investigations have been performed on the inverse system formed by depositing semiconductor thin films on metallic substrates.⁵⁻⁷ The reversal of the deposition sequence can significantly alter the chemical state and composition of the interface and have a significant influence on the interface morphology. It is important to investigate the geometrical structures of the interfaces formed by depositing semiconductors on metals in order to gain an understanding of the mechanisms that lead to these different structures.

In this paper, we report a study of thin films of germanium deposited under ultrahigh vacuum conditions on a single-crystal Ag(001) substrate. This system was chosen since several works on the adsorption of Ag on Ge (Refs. 1-3) have already been performed and also for comparison with the results of previous studies of the intermixing and phase segregation of metals on metals.⁸⁻¹⁰ In particular, the germanium-silver system is in some ways comparable to silver-copper in that (i) both tend to phase separation and (ii) the deposited element (Ge or Ag) has a lower surface free energy than the substrate (Ag or Cu, respectively).^{8,9,11} For the Ge/Ag system, it is also interesting to investigate whether the adsorbed Ge atoms behave like in a metal or a semiconductor. In metals the atoms usually tend to maximize the number of nearest neighbors in a close-packed structure. In semiconductors orbital hybridization leads to the formation of highly directional covalent bonds at the expense of the packing density.

A previous study by Auger electron spectroscopy (AES) and low-energy electron diffraction¹¹ (LEED) was devoted to the growth mode and the dissolution kinetics of Ge on Ag(001). It revealed in particular a sharp $p(2\sqrt{2}$

$\times 4\sqrt{2})R45^\circ$ superstructure up to about 0.5 ML coverage. The primary goal of the present paper is to clarify the atomic structure of the $p(2\sqrt{2}\times 4\sqrt{2})R45^\circ$ superstructure by combining surface x-ray diffraction (SXRD) and scanning tunneling microscopy (STM) studies.

II. EXPERIMENT

The experiments were performed at the Hamburg Synchrotron Radiation Laboratory (HASYLAB) at DESY, Germany. The samples were prepared in a large ultrahigh-vacuum system with extensive surface preparation and characterization facilities (e.g., reflection high-energy electron diffraction, LEED, STM, and x-ray fluorescence analysis). The Ag(001) substrates were cleaned by extended annealing and repeated cycles of sputtering with Ar⁺ ions (500 eV) and subsequent annealing at elevated temperatures (400–600 °C) until a sharp $p(1\times 1)$ LEED pattern was obtained. The germanium was deposited on the substrate at room temperature from a calibrated effusion cell with a pyrolytic boron nitride crucible at a pressure of 2×10^{-10} mbar. After depositing about 0.5 ML Ge (which corresponds to 6.0×10^{14} atoms/cm²) a sharp $p(2\sqrt{2}\times 4\sqrt{2})R45^\circ$ LEED pattern was obtained. Two nominally identical samples were prepared; one was used for the STM investigations and the other was transferred to a portable ultrahigh-vacuum chamber (base pressure less than 10^{-9} Torr) with a hemispherical Be window, which was mounted on the vertical diffractometer at the BW2 beamline at HASYLAB for the x-ray diffraction measurements. The x-ray wavelength was selected to be 1.33 Å using a silicon double-crystal monochromator. The angle of incidence was kept fixed at 0.4° (i.e., slightly larger than the critical angle for total reflection) during the measurements.

III. RESULTS

STM images have been recorded at various stages during the growth of Ge/Ag(001). Figure 1 is a filled-state atomically resolved STM image at 0.1 Ge ML on the well-ordered Ag(001) surface. We observe an isolated cluster with a

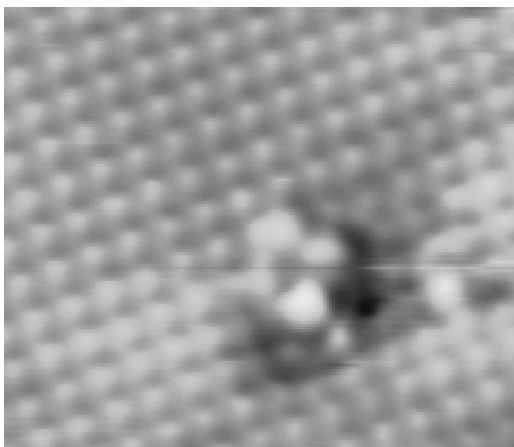


FIG. 1. Filled-state STM image ($4\text{ nm}\times 3\text{ nm}$ $V=-0.053\text{ V}$, $I=3.705\text{ nA}$) at $\sim 0.1\text{ ML}$ Ge coverage. An isolated group of four Ge atoms can be seen on the Ag(001) substrate.

slightly distorted square shape formed of four associated protrusions. This square is rotated 45° with respect to the $[10]$ direction of the silver surface. The interspacing between the protrusions is about $3.9\pm 0.5\text{ \AA}$.

Figure 2 shows a filled-state STM image of a $10\text{ nm}\times 10\text{ nm}$ area of the Ag(001) surface after the deposition of 0.5 ML Ge. The total gray scale of the image corresponds to a height amplitude of 0.5 \AA . This image shows wavy rows of spots that look like small clusters. The surface periodicity agrees with the $p(2\sqrt{2}\times 4\sqrt{2})R45^\circ$ superstructure observed in the LEED pattern. Figure 3 shows an atomic resolution STM image ($4\text{ nm}\times 4\text{ nm}$) of this superstructure; each spot of the former image is in fact made of four protrusions similarly to what is observed at 0.1 Ge ML . The maximum height difference between the protrusions does not exceed 0.1 \AA . Eight protrusions are observed in the unit cell with a glide line along the $[01]$ axis of the cell. It is appealing to consider the eight protrusions as Ge atoms, which would be consistent

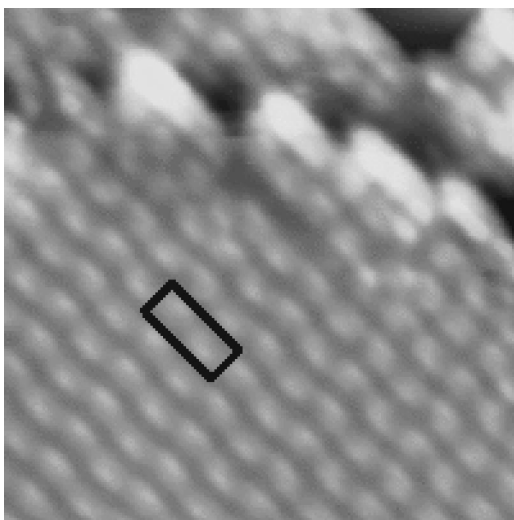
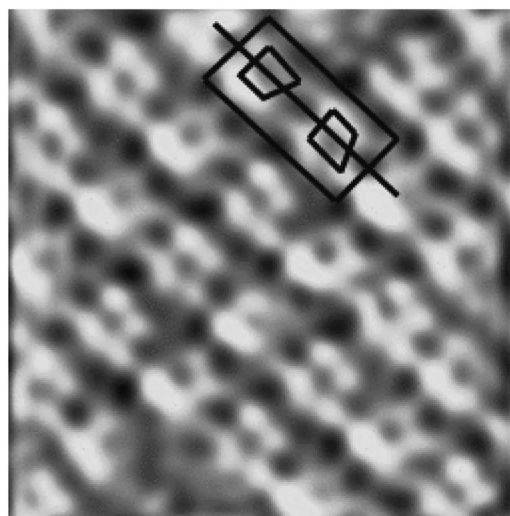
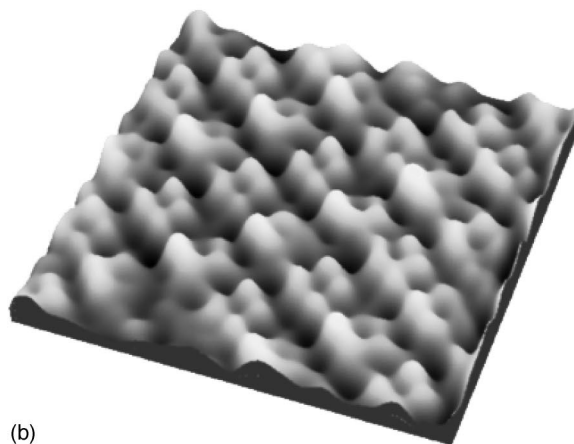


FIG. 2. Filled-state STM image ($10\text{ nm}\times 10\text{ nm}$ $V=-1.74\text{ V}$, $I=1.65\text{ nA}$) at 0.5 ML Ge coverage. The $[10]$ and $[01]$ directions of the silver surface are parallel to the sides of the image. Clusters (white protrusions) appear in the $p(2\sqrt{2}\times 4\sqrt{2})R45^\circ$ superstructure shown by a rectangle.



(a)



(b)

FIG. 3. Empty-state STM image ($4\text{ nm}\times 4\text{ nm}$ $V=0.004\text{ V}$, $I=8.64\text{ nA}$) showing an atomic resolution of the $p(2\sqrt{2}\times 4\sqrt{2})R45^\circ$ superstructure with two distorted tetramers in the surface unit cell. (a) top view, (b) 3D view. The unit-cell with the two Ge tetramers and its glide-mirror line are indicated in (a).

with the Auger calibration.¹¹ With this assumption, the STM images provide valuable information about possible starting models for the x-ray structure analysis.

The x-ray diffraction data consist of a set of 94 nonsymmetry-equivalent in-plane reflections and 6 nonsymmetry-equivalent rod profiles. Assuming equally populated domains the reciprocal space exhibits the $p4mm$ symmetry. The intensities of the in-plane reflections are shown by half circles in Fig. 4. The systematic error in the data set (17%) was estimated from the reproducibility of the most intense symmetry-equivalent reflections $[(3,0); (0,6); (-3,0); (0,-6)]$. In the reciprocal space basis (\vec{A}, \vec{B}) of the $p(2\sqrt{2}\times 4\sqrt{2})R45^\circ$ superstructure (see Fig. 4), the half-order reflections are missing along the h axis, which is consistent with the pg plane-group symmetry of the system.

Typical rod profiles are shown in Fig. 5. The modulation observed along the fractional order $(3/4, 3/4, l)$ rod results from the limited thickness of the reconstructed surface layer, which is roughly estimated to a few monolayers from the inverse width of this modulation. This qualitatively shows that the Ag atoms in the topmost layers are likely displaced

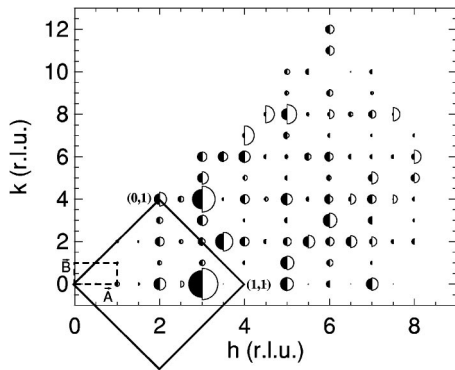


FIG. 4. Inplane SXRD intensities, measured (half circle on the right) and computed (half circle on the left). The areas of the circles are proportional to the intensities. The reflections are indexed (h, k) relatively to the reciprocal unit cell of the $p(2\sqrt{2} \times 4\sqrt{2})R45^\circ$ superstructure shown by the dashed rectangle. The solid line square represents the conventional LEED (1×1) reciprocal surface cell. The bulk Ag reflections indexed $(1,1)$, $(1,3)$, $(2,2)$, and $(0,2)$ in the conventional LEED notation are not represented due to their high intensities.

from the bulk silver lattice sites and therefore participate in the superstructure.

The structural analysis is based on the comparison of experimental and calculated data from simulations of the in-plane reflections and of the rod profiles using different models. Standard crystallographic data evaluation programs were used to analyze the data and determine the Ge and Ag atoms coordinates. The refinement of the atomic positions in the model is performed by minimizing the usual χ^2 parameter allowing the Debye-Waller terms, and an appropriate scale-

factor to vary. The preliminary analysis relies on the in-plane fractional order reflections, which are sensitive to the structure projected on the surface plane; subsequent analysis of the rod profiles reveals the full three-dimensional structure.

We investigated several models with the pg symmetry as indicated by the missing reflections in the SXRD and LEED data and the atomic resolution STM images. This symmetry requires that the number of Ge atoms in the $p(2\sqrt{2} \times 4\sqrt{2})R45^\circ$ unit cell is even. The uncertainty in the AES calibration¹¹ allows unit cells with 8 ± 2 Ge atoms and the STM images suggest a unit cell with 8 atoms. On this basis, we have studied models with

- (i) 6, 8 and 10 Ge adatoms,
- (ii) 6, 8 and 10 substitutional Ge atoms in the Ag top layer.

Vacancies in the first Ag layer were also considered in these trial models.

The models with substitutional Ge atoms are definitely ruled out since χ^2 cannot be reduced less than 3.9. The best fits are obtained for models with eight Ge adatoms. In the data analysis, a large number of configurations have been tested with the four Ge atoms of the asymmetric half-unit cell initially located in hollow, bridge or top sites of the Ag surface. In a first stage, the refinement of the positions of the Ge adatoms and the Ag atoms in the first layer gives a χ^2 factor of 2.3. The fit is further improved by relaxing the atoms in the second Ag layer. The final χ^2 is equal to 0.9.

Figures 4 and 5 show the best fit simulations along with the experimental in-plane reflections and rod profiles. The proposed model is presented in Fig. 6 and the atomic coordinates of the four Ge atoms of the asymmetric unit in the surface layer are given in Table I. Rows of Ge adatoms par-

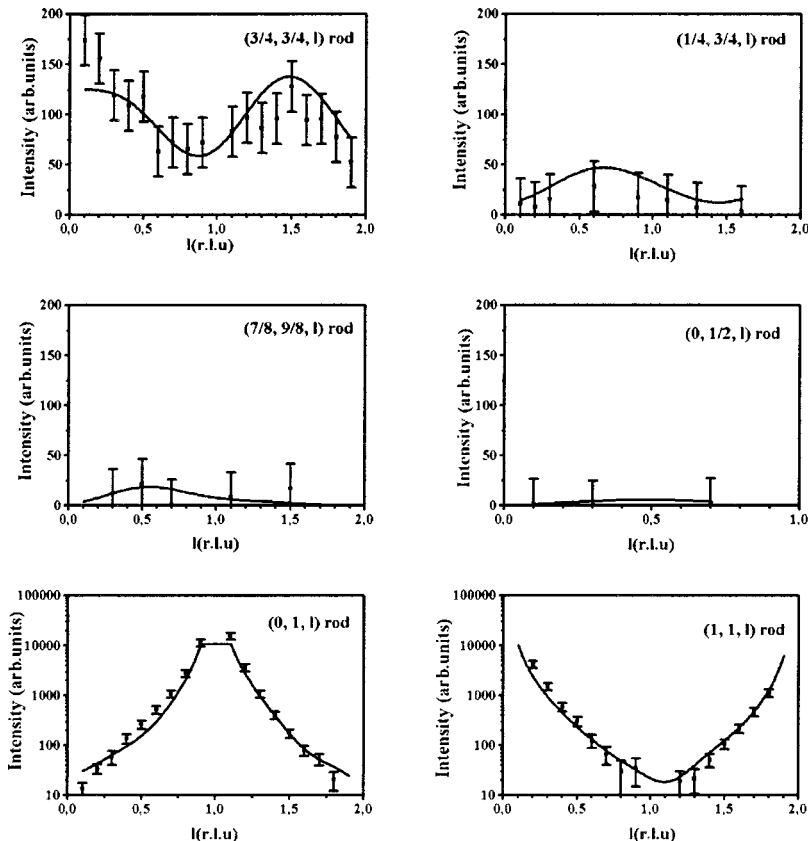


FIG. 5. Rod profiles for 6 nonequivalent fractional (upper rows) and integer order (lower row) reflections. The indices are given with the LEED convention. Data and best fit are shown by the symbols and the solid lines, respectively.

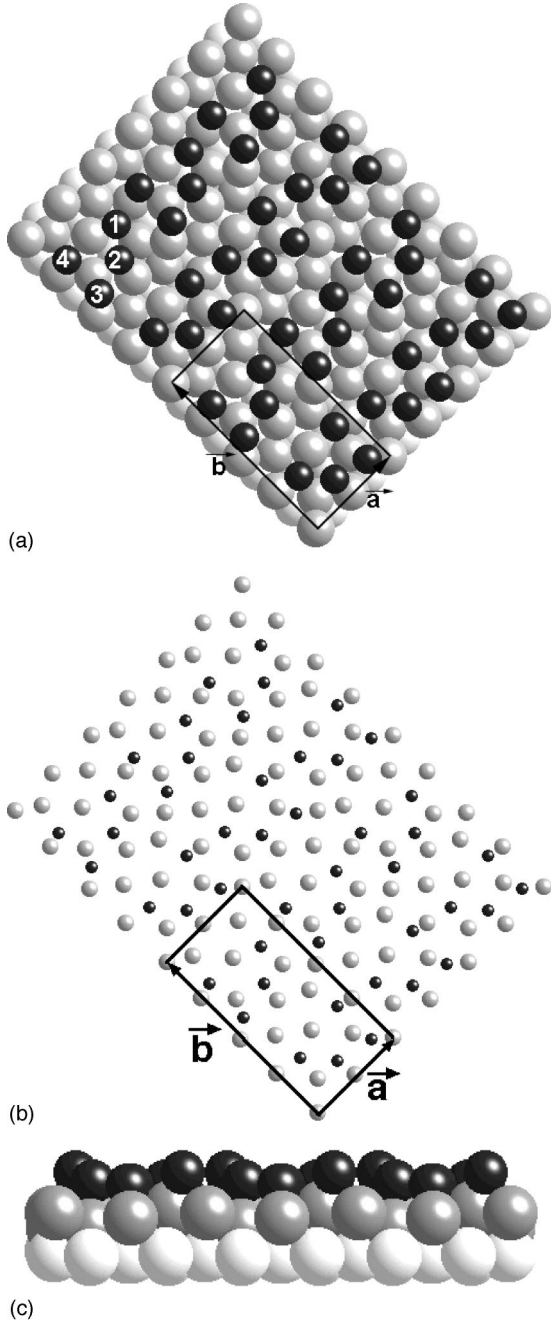


FIG. 6. The proposed model for the $p(2\sqrt{2}\times 4\sqrt{2})R45^\circ$ superstructure; Atomic coordinates of the Ge atoms are given in Table I. (a) top view and (c) side view normal to the $[01]$ direction. Black circles represent the Ge atoms and the dark and light-grey circles the Ag atoms in the first and second layer, respectively. (b) Detailed image of the proposed atomic structure of the $p(2\sqrt{2}\times 4\sqrt{2})R45^\circ$ reconstruction outlining the local environment of the Ge atoms (dark circles). The Ag atoms in the first layer are represented in shadowed grey.

allel to the $[10]$ direction of the $p(2\sqrt{2}\times 4\sqrt{2})R45^\circ$ cell are clearly visible. There are two rows of 4 Ge atoms per unit cell in agreement with the pg group symmetry. In these Ge tetramers, the atoms are located near hollow [atoms labeled 1, 2, and 4 in Fig. 6(a)] or bridge (atom 3) adsorption sites of the $\text{Ag}(001)$ surface. The Ge height positions (0.139 to 0.252 nm) above the average underlying Ag plane reveal a rather

TABLE I. Atomic coordinates of the 4 nonequivalent Ge atoms in the $p(2\sqrt{2}\times 4\sqrt{2})R45^\circ$ unit cell ($a=0.817$ nm, $b=1.634$ nm); x and y are relative coordinates whereas z denotes the Ge atom height above the average Ag top layer. The coordinates of the other four Ge atoms are given by the symmetry relation: $1-x, y+1/2$.

#	x	y	$z(\text{nm})/\text{Ag surface}$
1	0.853 ± 0.005	0.052 ± 0.003	0.252 ± 0.004
2	0.846 ± 0.005	0.275 ± 0.003	0.139 ± 0.004
3	0.486 ± 0.005	0.095 ± 0.003	0.180 ± 0.004
4	0.258 ± 0.005	0.229 ± 0.003	0.205 ± 0.004

large surface corrugation, which can be seen in the side view of Fig. 6(c). The lateral displacements of the Ag atoms in the first layer can be more clearly seen in Fig. 6(b). The root-mean square displacement and the relaxation of the two top Ag layers are given in Table II. Significant displacements of the Ag atoms are shown, more particularly in the $[01]$ surface direction resulting in a slightly higher silver atomic surface density underneath the Ge tetramers. The mean square displacement of the Ag atoms is also important normal to the surface in agreement with the rather large corrugation of the Ge surface layer. The displacements are smaller in the second layer than in the first one. The Debye-Waller parameters used for the best fit for Ge and Ag in the first and second layers and in the bulk, are 3.2, 5.4, 1.7, and 0.5 \AA^2 , respectively. The large values of the surface Debye-Waller factors and particularly for the first Ag layer are indicative of multiple positions, which cannot be resolved from the present data.

IV. DISCUSSION

The comparison of the atomically resolved STM images with the top layer arrangement deduced from the SXR analysis (Figs. 3 and 6) reveals a fairly good agreement about the structure of 0.5 Ge ML on $\text{Ag}(001)$. Both techniques show (i) the $p(2\sqrt{2}\times 4\sqrt{2})R45^\circ$ reconstruction with the pg symmetry and (ii) the existence of two Ge tetramers per unit cell. Although tetramers with similar shape and the same orientation on the (001) surface are evidenced by both STM and SXR, a more extended detailed comparison of the Ge atomic coordinates reveals small discrepancies, which may originate from the different ranges of order, local range and long range, respectively. In addition the ability for STM to provide the actual atomic image of the surface may be questioned.

TABLE II. Root mean square (rms) displacements of the Ag atoms of the two top layers in the $[10]$ ($\sqrt{\langle \Delta X^2 \rangle}$) and $[01]$ ($\sqrt{\langle \Delta Y^2 \rangle}$) surface directions of the $p(2\sqrt{2}\times 4\sqrt{2})R45^\circ$ superstructure, and perpendicularly ($\sqrt{\langle \Delta Z^2 \rangle}$). The average relaxation is given by $\langle \Delta Z \rangle$.

#	$\sqrt{\langle \Delta X^2 \rangle}$ (nm)	$\sqrt{\langle \Delta Y^2 \rangle}$ (nm)	$\sqrt{\langle \Delta Z^2 \rangle}$ (nm)	$\langle \Delta Z \rangle$
1st Ag layer	0.013 ± 0.004	0.038 ± 0.004	0.039 ± 0.004	-4%
2nd Ag layer	0.010 ± 0.004	0.015 ± 0.004	0.019 ± 0.004	-0.1%

A recent calculation¹² of the electronic structure of the Ge/Ag(001) system has shown that the density of states at the Fermi level has maxima at the actual positions of the surface atoms. This would suggest that the STM images would not be dominated by electronic effects and would provide steric geometric views of the surface. This calculation however ignores the tip-surface electronic interactions, which could alter more or less heavily the images.

The SXR D model shows that the Ge atoms are located in the close vicinity of the preferential hollow or bridge sites of the Ag(001) surface. Using an *ab initio* full-potential linear muffin-tin orbital approach, Sawaya *et al.*¹² have shown a strong preference for isolated Ge adatoms to adsorb on hollow sites. It is worth noting that the bridge surface sites are energetically the second most favorable sites. In addition, Sawaya *et al.* claim that the adsorption characteristics are practically coverage independent. The calculation suggests that at half monolayer, Ge atoms may adsorb either on hollow or on bridge sites, in qualitative agreement with the experimental results presented above. The calculations do not allow any reconstruction of the Ag(001) surface. A more detailed comparison between theory and experiment is therefore not possible.

The Ge-Ge interatomic distances in the unit cell are $d_{12}=0.287\pm 0.004$ nm, $d_{23}=0.316\pm 0.004$ nm, $d_{34}=0.351\pm 0.004$ nm, and $d_{14}=0.382\pm 0.004$ nm, respectively [see Fig. 6(a)]. Only d_{12} is close to the Ge-Ge bond length in the three-dimensional (3D) diamondlike Ge structure (0.245 nm); all the others are significantly larger. In addition, the height distribution of the Ge atoms in the SXR D model shows that the tetramers are not planar. The proposed model, in fact, reveals the competition between the tendency to forming short and oriented Ge-Ge bonds and that of adsorbing Ge in preferential Ag surface sites.

The stability of the Ge tetramers observed in the $p(2\sqrt{2}\times 4\sqrt{2})R45^\circ$ reconstruction is also supported by their existence at lower coverage (Fig. 1). Moreover, a previous study¹¹ has shown a rapid dissolution of Ge upon annealing 1 ML Ge/Ag(001) at 250 °C, which stops when the $p(2\sqrt{2}\times 4\sqrt{2})R45^\circ$ superstructure is attained at 0.5 Ge ML coverage.

The bonding between the Ge atoms and the Ag atoms induces subsurface displacements, which involve the two top atomic layers and produces a density modulation in the substrate. The 4% inward relaxation of the first Ag layer is not untypical for this type of metallic surface [about 3% was reported for the clean Ag(001) surface.¹³] The disorder in the top Ag layers indicated by the larger Debye-Waller factors deduced from the SXR D analysis indicates that the $p(2\sqrt{2}\times 4\sqrt{2})R45^\circ$ phase may be a precursor to the surface modification observed by AES-LEED at higher Ge coverages.¹¹ We expect the structure induced by Ge on Ag(001) to be driven by a delicate balance between surface-substrate lattice mismatch, bond enhancement, and stress relaxation, representative of the relative strengths of Ag-Ag, Ge-Ge, and Ag-Ge bonds. For relatively weak Ge-Ge interactions one would expect Ge atoms to occupy favorable adsorption sites

on the unperturbed Ag(001) surface. On the other hand, stronger Ge-Ge interactions would produce Ge clusters on top of an essentially unperturbed Ag(001) surface if the Ge-Ag bonds were weak. The reconstruction of the Ag(001) surface layers shown in the present work suggests that both the Ge-Ge and Ge-Ag interactions play a significant role in this system. It is known that the clean Ag(001) surface does not reconstruct, whereas its iso-electronic neighbor in the 5d series, Au(001), forms a contracted quasi-hexagonal top layer on the underlying square lattice.^{14,15} The Au(001) reconstruction¹⁶ is attributed to the gain in the number of nearest neighbor bonds rather than to stress relief. Theoretical calculations¹⁷ indicate that the top layer of clean Ag(001) would prefer to transform into a more compact hexagonal arrangement, but the energy gain is not sufficient to overcome the substrate potential that pins the top layer. Ge adsorption on Ag(001) could favor the natural tendency of silver to pack more closely, locally in rows of higher atomic density.

The Ge/Ag system was primarily chosen for its similarities with the bimetallic Ag/Cu system concerning its tendency to phase separation and the lower surface tension of the deposit in both systems. These properties easily justify that the Ge atoms do not incorporate in the Ag(001) surface. More original is the stabilization of the Ge clusters at 0.5 ML, which has no equivalent for Ag/Cu. The formation of Ge tetramers is likely responsible for the particularly stable $p(2\sqrt{2}\times 4\sqrt{2})R45^\circ$ superstructure. Ge/Ag(001) can be finally considered as representative of a new class of binary systems different from the bimetallic ones previously observed.

V. SUMMARY

An atomic model deduced from STM and SXR D studies is presented for the $p(2\sqrt{2}\times 4\sqrt{2})R45^\circ$ superstructure induced by 0.5 ML Ge deposited on an Ag(001) single-crystal substrate. The model is made up of two Ge atom tetramers per unit cell on top of a reconstructed Ag bilayer. Ge adsorption induces displacements of the Ag atoms in the top two layers resulting in a density modulation. The Ge atoms are preferentially adsorbed near hollow and bridge sites of the Ag(001) substrate.

ACKNOWLEDGMENTS

We thank the staff of HASYLAB for their technical assistance. Financial support from the Bundesministerium für Bildung, Wissenschaft, Forschung und Technologie (BMBF) under Project No. 05 SB8 GUA6 and the Volkswagen Stiftung is gratefully acknowledged. The work at the HASYLAB was supported in part by the European Community through the TMR program. The authors gratefully acknowledge J.P. Bibérian, J. Goniakowsky, A. Saúl, S. Sawaya, and G. Trégliá for fruitful discussions. The CRMC² is also associated with the Universities of Aix-Marseille II and III.

- ¹C. Collazo-Davila, D. Grozea, L. D. Marks, R. Feidenhans'l, M. Nielsen, L. Seehofer, L. Lottermoser, G. Falkenberg, R. L. Johnson, M. Göthelid, and U. Karlsson, *Surf. Sci.* **418**, 395 (1998).
- ²A. L. Wachs, T. Miller, and T.-C. Chiang, *Phys. Rev. B* **33**, 8870 (1986).
- ³M. Hammar, M. Göthelid, U. O. Karlsson, and S. A. Flodström, *Phys. Rev. B* **47**, 15 669 (1993).
- ⁴D. Grozea, E. Landree, L. D. Marks, R. Feidenhans'l, M. Nielsen, and R. L. Johnson, *Surf. Sci.* **32**, 418 (1988).
- ⁵J. A. Martìn-Gago, R. Fasel, J. Hayoz, R. G. Agostino, D. Naumović, P. Aebi, and L. Schlapbach, *Phys. Rev. B* **55**, 12 896 (1997).
- ⁶R. Dudde, H. Bernhoff, and B. Reihl, *Phys. Rev. B* **41**, 12 029 (1990).
- ⁷C. Polop, J. L. Sacedon, and J. A. Martìn-Gago, *Surf. Sci.* **402**, 245 (1998).
- ⁸J. Eugène, B. Aufray, and F. Cabané, *Surf. Sci.* **241**, 1 (1991).
- ⁹Y. Liu and P. Wynblatt, *Surf. Sci.* **240**, 245 (1990).
- ¹⁰H. Giordano, O. Alem, and B. Aufray, *Scr. Metall. Mater.* **28**, 257 (1993).
- ¹¹H. Oughaddou, B. Aufray, J. P. Bibérian, and J. Y. Hoarau, *Surf. Sci.* **429**, 320 (1999).
- ¹²S. Sawaya, J. Goniakowski, and G. Trégliá, *Phys. Rev. B* **59**, 15 337 (1999).
- ¹³C. T. Chan, K. M. Ho, and K. P. Bohnen, in *Handbook of Surface Science Volume 1*, edited by W. N. Unertl (Elsevier Science, New York, 1996), p. 101; K. P. Bohnen and K. M. Ho, *Surf. Sci. Rep.* **19**, 99 (1993).
- ¹⁴M. A. van Hove, R. J. Koestner, P. C. Stair, J. P. Bibérian, L. L. Kesmodel, I. Bartos, and G. A. Somorjai, *Surf. Sci.* **103**, 189 (1981).
- ¹⁵Y. F. Liew and G. C. Wang, *Surf. Sci.* **227**, 190 (1990).
- ¹⁶H. Ibach, *Surf. Sci. Rep.* **29**, 193 (1997).
- ¹⁷N. Takeuchi, C. T. Chan, and K. M. Ho, *Phys. Rev. Lett.* **63**, 1273 (1989).